



Published in final edited form as:

J Comput Assist Tomogr. 2018 ; 42(4): 601–606. doi:10.1097/RCT.0000000000000727.

Malignant Pleural Mesothelioma: Are There Imaging Characteristics Associated with Different Histologic Subtypes on Computed Tomography?

Joanna G. Escalon, MD^a, Kate A. Harrington, MB, BCh, BAO^a, Andrew J. Plodkowski, MD^a, Junting Zheng, MS^a, Marinela Capanu, PhD^a, Marjorie G. Zauderer, MD^a, Valerie W. Rusch, MD^a, Michelle S. Ginsberg, MD^{*a}

Joanna G. Escalon: joannagescalon@gmail.com; Kate A. Harrington: harringtonkatea@gmail.com; Andrew J. Plodkowski: plodkova@mskcc.org; Junting Zheng: zhengj@mskcc.org; Marinela Capanu: capanum@mskcc.org; Marjorie G. Zauderer: zauderem@mskcc.org; Valerie W. Rusch: ruschv@mskcc.org; Michelle S. Ginsberg: ginsberm@mskcc.org

^aMemorial Sloan Kettering Cancer Center, 1275 York Ave, New York, NY 10065, USA

Abstract

Objectives—Determine imaging characteristics specific to epithelioid (eMPM), sarcomatoid (sMPM), and biphasic (bMPM) subtypes of malignant pleural mesothelioma (MPM) on computed tomography (CT).

Methods—Preoperative CT scans of patients with MPM were retrospectively assessed for numerous features including primary affected side, volume loss, pleural thickness, pleural calcifications, pleural effusion, and lymphadenopathy.

Results—125 patients with MPM were included. Histologic subdivision was 97 eMPM (77%), 17 bMPM (14%), and 11 sMPM (9%). Non-epithelioid MPM (bMPM and sMPM) was more likely than eMPM to have calcified pleural plaques ($P=0.035$). Analyzed separately, bMPM and sMPM each demonstrated calcified plaques more frequently than eMPM, and sMPM more often had internal mammary nodes; however, P -values did not reach significance ($P=0.075$ and 0.071 , respectively).

Conclusions—Calcified plaques are significantly more common in non-epithelioid subtypes compared to eMPM. Given the different prognoses and management of MPM subtypes, accurate non-invasive subtype classification is clinically vital.

Keywords

Mesothelioma; Epithelioid; Sarcomatoid; Biphasic; Computed Tomography

INTRODUCTION

Malignant pleural mesothelioma (MPM) is a rare neoplasm with an annual incidence in the United States of 2500 cases.¹ Nevertheless, it is the most common primary malignancy of the pleura and has been increasing in incidence in recent decades in the US and worldwide,

*Corresponding Author: Joanna G. Escalon, M.D., 1275 York Ave, New York, NY 10065, USA, joannagescalon@gmail.com.

related to an increase in asbestos exposure in industrialized countries.² Prognosis remains overall poor with a median survival of 9-17 months.¹ Multimodality therapy comprised of surgery and subsequent chemoradiation can prolong survival.^{3,4}

Histologic subtype is a strong prognostic factor and key for treatment planning. MPM is divided by cellular morphology into three broad histologic subtypes: epithelioid, sarcomatoid, and biphasic/mixed. Epithelioid MPM (eMPM) is the most common subtype, representing approximately 70% of all cases. Sarcomatoid MPM (sMPM) accounts for 10% of cases and biphasic MPM (bMPM), which consists of a mixture of at least 10% of both epithelioid and sarcomatoid components, accounts for the remainder.⁵ Epithelioid histology has the longest survival, sarcomatoid has the worst, and biphasic has an intermediate survival.⁶ One 2015 study of 1183 patients with MPM found a median survival of 14 months, 10 months, and 4 months in the epithelioid, biphasic and sarcomatoid groups, respectively.⁷⁻⁹

Computed tomography (CT) is the primary modality for identifying and evaluating patients with MPM. The majority of patients demonstrate a unilateral pleural effusion (74%) and pleural thickening (92%).¹⁰ Pleural thickening that is nodular, lobular, circumferential or greater than 1 cm in thickness is particularly concerning for MPM.^{1,11} Additional common imaging findings detectable by CT include ipsilateral volume loss, invasion of the pericardium, mediastinum, diaphragm or chest wall, intrathoracic nodal involvement, and pulmonary and distant metastases.^{1,12} Local tumor extension into the chest wall, diaphragm, mediastinum, or spine often manifests as obscured fat planes and precludes surgical resection.

In 1981, Alexander et al published one of the earliest papers describing the CT findings of mesothelioma [Alexander].¹³ To this date, however, given the rarity of the disease, no large series exists describing the CT appearance of different subtypes of mesothelioma. Given that histological subtype consistently correlates with overall survival, finding a reliable way to distinguish these subtypes in patients with MPM would be extremely helpful in triaging patients, particularly those who have diagnoses made on small biopsies (e.g. fine needle biopsy or pleural fluid cytology) rather than surgical biopsies. Surgeons and Oncologists can then use this information to plan management, stratify patients in clinical trials, and help families and patients make informed decisions. Three identified studies address whether CT characteristics can be used to reliably distinguish the histologic subtypes of mesothelioma, but all have conflicting results.¹⁴⁻¹⁶

We present a retrospective study similarly analyzing CT features of these distinct subtypes to identify any potential differentiating characteristics. The current study uniquely uses pathology predominantly from surgical resection (pleurectomy decortication, extrapleural pneumonectomy, exploratory thoracotomy, wedge resection or lobectomy) with a small percentage from video-assisted thoracoscopic surgery biopsy, thus providing a uniform and reliable classification of all patients. We aim to provide some clarity on the issue given the conflicting results of prior research.

MATERIAL AND METHODS

Imaging Review

Our institutional review board approved this retrospective study and waived the requirement for informed consent. This study was Health Insurance Portability and Accountability compliant. Consecutive patients were identified from a prospectively maintained institutional database of patients with a pathologic diagnosis of MPM who underwent resection or open pleural biopsy, diagnosed from January 10, 2005 to October 23, 2015. Patients were excluded based on defined imaging and pathologic criteria. Specifically, all patients had to have a contrast-enhanced digital CT within 90 days of surgery, no history of pleurodesis at the time of the CT, and MPM on final pathology.

The images were reviewed on a picture archiving and communications system (GE PACS; Waukesha, WI). Many of the patients had been referred from outside institutions to our tertiary referral center following initial imaging elsewhere; therefore, CT protocols varied slightly. Initial staging CT scans were performed on a range of multi-detector CT scanners, with slice thickness varying from 1.25 to 7.5 mm with the majority having a slice thickness 5 mm (n= 111, 89%). The majority of cases were only available in the axial plane (n= 73, 58%), while the remainder had coronal or sagittal reformats available for review (n= 52, 42%). All patients had contrast-enhanced CT scans.

All imaging was independently reviewed by two trainees, post-graduate years 5 and 8, blinded to the patient's pathology. Discordant findings were reviewed by two thoracic attendings and final assessment determined by consensus.

Each CT was assessed for primary affected side, presence of volume loss, pleural calcifications, pleural effusion, pulmonary nodules, and thoracic lymphadenopathy. Pleural thickening was graded as continuous or discontinuous and lobulated or smooth (Figures 1–2). Maximum pleural thickness was measured in the upper lung (defined as above the carina), lower lung (defined as below the carina), and along the diaphragm, also noting the location of the maximum pleural thickening at each level (paramediastinal, paraspinal, or lateral). Pleural thickening was measured on the lung windows. Soft tissues windows were used for confirmation and to ensure the area of suspected pleural thickening was soft tissue rather than fluid density. Volume loss was assessed subjectively by the radiologist. If a PET-CT or CT of the abdomen and pelvis was available within 1 month of the index scan, the imaging and report if available were reviewed to assess for distant metastases.

Pathology Review

Pathologic diagnosis was obtained from the surgical database. All surgery was performed at the same tertiary care center and pathology reviewed by in house pathologists who specialized in thoracic malignancies.¹⁷

Statistics

Associations between pathologic subtypes and categorical features were assessed using Fisher's exact test while the Kruskal-Wallis test was used to test for differences in

continuous CT characteristics between the subtypes. P-values of <0.05 were considered significant.

RESULTS

289 subjects with MPM were identified from a surgical database spanning 10 years. Seventy-five subjects were excluded due to lack of a preoperative contrast-enhanced CT scan available in our system (50) or only available as a hardcopy (25). Twenty-nine subjects were excluded due to a greater than 90 days between the index preoperative contrast enhanced CT scan and surgery. Fifty-five subjects were removed due to evidence of prior talc pleurodesis, subsequently confirmed in the medical record, which was felt would affect CT imaging characteristics. Five subjects were removed from study due to final pathology yielding benign (2), non-classifiable (2), or non-mesothelioma (1) results.

After all exclusions, 125 patients (99:26 M:F, mean age 69) with MPM underwent imaging evaluation with CT performed an average of 31 (range 1–87) days before surgical resection or open pleural biopsy. The histologic subdivisions were epithelioid (77%, 97 of 125), biphasic (14%, 17 of 125), and sarcomatoid (9%, 11 of 125). 90% of subjects were determined to have a clinical stage of 2 or higher (Table 1). Pathology was obtained from one of the following procedures: pleurectomy decortication (P/D, 43%, 54 of 125), extrapleural pneumonectomy (EPP, 24%, 30 of 125), exploratory thoracotomy (15%, 19 of 125), video-assisted thoracoscopic surgery biopsy (VATS, 14%, 18 of 125), or wedge resection or lobectomy (3%, 4 of 125).

There was no significant difference in degree, location, or appearance of pleural thickening seen on CT between the three histologic subtypes (Table 1). In evaluation of additional ancillary characteristics, there was no significant difference between histologic subtypes (Table 2, Figures 3–4). bMPM and sMPM were more likely to demonstrate calcified pleural plaques and sMPM with internal mammary nodes with P-values approaching significance ($P = 0.075$ and 0.071 , respectively). Calcified plaques were seen in 24 of 97 (25%) eMPM, 7 of 17 (41%) bMPM, and 6 of 11 (55%) sMPM. Internal mammary nodes were seen in 21 of 97 (22%) eMPM, 4 of 17 (24%) bMPM, and 6 of 11 (55%) sMPM.

While imaging correlates were not statistically significantly associated with the three histologic subtypes, using the binary categorization from the CALGB prognostic index of epithelioid versus non-epithelioid subtypes, repeat analysis was performed comparing epithelioid MPM and all non-epithelioid MPM (grouping biphasic and sarcomatoid together).⁸ In this analysis, bMPM and sMPM combined were more likely to have calcified plaques than eMPM ($P = 0.035$). When stratified analysis accounting for differences in clinical stage was performed, both calcified plaques and local invasion were found to be more common in non-epithelioid subtype compared to eMPM. Calcified plaques were present in 13/28 (46%) of the non-epithelioid group compared to 24/97 (25%) of eMPM ($P = 0.058$). Local invasion was present in 20/28 (71%) of the non-epithelioid group compared to 50/97 (52%) of eMPM ($P = 0.045$). There was no significant difference in characterization of pleural thickening or other ancillary findings on CT.

DISCUSSION

Given the different management strategies between histologic subtypes of MPM and consistent correlation of histologic subtype with overall survival, finding a reliable way to distinguish these subtypes would be extremely helpful in triaging patients, particularly those who have diagnoses made on small biopsies (e.g. fine needle biopsy or pleural fluid cytology) rather than surgical biopsies. Identifying eMPM from non-epithelioid subtypes would prove most useful as eMPM has the best prognosis and is the most appropriate for surgery. This would give surgeons and oncologists more confidence in recommending aggressive trimodality therapy for these patients and diverting higher risk patients to more experimental interventions. CT imaging is the primary modality for identifying and evaluating patients with MPM and would be the easiest non-invasive means to classify subtypes. However, prior studies have shown conflicting results regarding which CT characteristics could be used for subtype differentiation.

In 2000, Senyigit et al evaluated the imaging features of 117 patients with mesothelioma and found that sarcomatoid subtype was more likely to involve the mediastinal pleura, inter-lobar fissures, and lung parenchyma.¹⁴ In 2009, Seely et al assessed the CT appearances of 92 patients with mesothelioma, composed of 72 (78%) epithelioid, 15 sarcomatoid (16%) and 5 (5%) biphasic type. The only statistically significant difference between the groups was the more frequent presence of ipsilateral volume loss in sarcomatoid and biphasic mesothelioma.¹⁵ However, in 2015, Dickens et al performed a similar study in which they assessed 139 patients with mesothelioma, 96 (69%) epithelioid subtype, 25 (18%) sarcomatoid, 9 (7%) biphasic, and 9 (7%) unclassified. They found no difference in frequency of volume loss between the groups, but noted that epithelioid type more commonly demonstrated a simple pleural effusion and sarcomatoid type more often presented as a focal mass.¹⁶

In our study, we found that combined non-epithelioid subtypes are more likely to have calcified plaques than eMPM ($P = 0.035$). Additionally, calcified pleural plaques appear more common in bMPM and sMPM when analyzed separately compared to eMPM and internal mammary nodes were more common in sMPM. When stratified analysis accounting for differences in clinical stage was performed, both calcified plaques and local invasion were found to be more common in non-epithelioid subtype compared to eMPM ($P = 0.057$ and 0.045 , respectively).

Our study is unique in obtaining histologic subtype classification primarily from surgical resection rather than less accurate techniques such as transthoracic biopsy in a large cohort of patients with this rare tumor. Open pleural biopsy is the most accurate sampling method and considered the gold standard diagnosis of MPM.¹⁸ All other pleural biopsy options are all less sensitive for determining histologic subtype, particularly non-epithelioid subtypes. One study reviewing patients who had undergone thoracotomy, thoracoscopy, or CT-guided procedure followed by EPP, found an overall subtype misclassification rate of 20%.¹⁹ Image-guided transthoracic biopsy has the lowest accuracy in subtype classification (44%) when compared to thoracoscopy (74%) and thoracotomy (83%).¹⁹ Open pleural biopsy demonstrates a sensitivity and specificity for epithelioid MPM of 97% and 56%,

respectively. In contrast, the sensitivity and specificity of open pleural biopsy for non-epithelioid subtypes were 56% and 97%, respectively, and the positive and negative predictive values were 91% and 79%, respectively.¹⁸ These studies demonstrate that pre-resection biopsy has a high rate of subtype misclassification, particularly for non-epithelioid subtypes, with open biopsy being notably more accurate than transthoracic image-guided biopsies.

In our study, 100% of pathology diagnoses were obtained from a surgical procedure (as detailed in the results section); none were obtained by image-guided biopsies. Moreover, 67% of our patient's underwent complete surgical resection by pleurectomy decortication or extrapleural pneumonectomy. This is in contrast to prior studies in which the vast majority of specimens were from either surgical biopsy or image-guided biopsies, thus introducing a probable higher rate of misclassification of histologic subtype. As most studies are relatively small sample size, misclassification of patients can presumably have a significant effect on findings. We also excluded all patients with prior pleurodesis, which could alter CT findings.

It must be noted that CT is limited in its ability to predict lymph node involvement and can underestimate extent of disease in early chest wall involvement. However, ongoing work suggests volumetric CT may provide more accurate clinical staging.^{20,21} Positron emission tomography (PET)-CT has increased accuracy in detecting nodal metastases and occult extrathoracic metastases as well as for localizing metabolically active biopsy targets. Additionally, preliminary data suggest that FDG avidity within epithelioid mesothelioma may help identify rare pleomorphic subtype, which has a poorer prognosis.²² Magnetic Resonance Imaging (MRI) has been shown to be superior to CT in specifically detecting a single focus of chest wall invasion and in identifying invasion of the diaphragm or the endothoracic fascia.³ One study by Gill et al in 2009 evaluated the use of diffusion-weighted MRI to distinguish between histologic subtypes and found apparent diffusion coefficient (ADC) values of epithelioid mesothelioma to be higher than those of sarcomatoid and biphasic with the latter two histologies demonstrating similar ADC values. However, the authors point out that use of MRI in this patient population may be limited by inability to perform breath-hold, which subjects the study to errors in ADC due to image misregistration.²

The retrospective nature of our study and its relatively small sample size are inherent limitations, both of which could be overcome by larger prospective multi-institutional studies. We also had a relatively small number of nonepithelioid MPM cases, although this is similar to the distribution in prior studies and reflecting the lower incidence of this subtype. From a statistically perspective, due to the exploratory and hypothesis generating nature of the study, multiple testing was not employed and p-values < 0.05 were considered significant, and thus the results need to be interpreted with caution and validated in future studies.

In summary, our study shows that calcified pleural plaques and local invasion are more common in non-epithelioid subtypes of MPM compared to eMPM. Prior studies have shown conflicting results as to whether the histologic subtypes of MPM can be reliably distinguished by CT characteristics. Our study is unique in obtaining histologic subtype

classification primarily from surgical resection, which is more accurate. Accurate non-invasive identification of eMPM is clinically vital, not simply academic. These patients typically undergo surgery in the setting of aggressive trimodality therapy in the United States, while higher risk patients, particularly those with sMPM, are diverted to more experimental interventions. Accurate subtype classification allows surgeons and oncologists to confidently recommend the appropriate treatment pathway. Further studies with larger cohorts may be useful to confirm the use of CT characteristics in distinguishing epithelioid from non-epithelioid histologies.

Acknowledgments

The authors would like to thank Joanne Chin and Sumar Hayan for assisting with the preparation of the manuscript.

This research was funded in part through the NIH/NCI Cancer Center Support Grant P30 CA008748. The funding source had no involvement in study design; in the collection, analysis and interpretation of data; in the writing of the report; or in the decision to submit the article for publication.

Conflicts of Interest and Source of Funding

All authors were partially supported by NIH/NCI Cancer Center Support Grant P30 CA008748. Marjorie G. Zauderer consulted for Astra Zeneca and Sellas Life Sciences and institution receives research funding from Verastem, MedImmune, Epizyme, Polaris, Sellas Life Sciences, and Bristol-Myers Squibb. Valerie W. Rusch is an unpaid member of the BMS Mesothelioma Scientific Advisory Board.

References

1. Nickell LT Jr, Lichtenberger JP 3rd, Khorashadi L, et al. Multimodality imaging for characterization, classification, and staging of malignant pleural mesothelioma. *Radiographics : a review publication of the Radiological Society of North America, Inc.* 2014; 34:1692–706.
2. Gill RR, Umeoka S, Mamata H, et al. Diffusion-weighted MRI of malignant pleural mesothelioma: preliminary assessment of apparent diffusion coefficient in histologic subtypes. *AJR American journal of roentgenology.* 2010; 195:W125–30. [PubMed: 20651171]
3. Wang ZJ, Reddy GP, Gotway MB, et al. Malignant pleural mesothelioma: evaluation with CT, MR imaging, and PET. *Radiographics : a review publication of the Radiological Society of North America, Inc.* 2004; 24:105–19.
4. Koyuncu A, Koksall D, Ozmen O, et al. Prognostic factors in malignant pleural mesothelioma: a retrospective study of 60 Turkish patients. *Journal of cancer research and therapeutics.* 2015; 11:216–22. [PubMed: 25879365]
5. van Zandwijk N, Clarke C, Henderson D, et al. Guidelines for the diagnosis and treatment of malignant pleural mesothelioma. *Journal of thoracic disease.* 2013; 5:E254–307. [PubMed: 24416529]
6. Churg, A, Roggli, V, F, G-S. Mesothelioma. In: Travis, WD, B, E, Muller-Hermelink, HK. , et al., editors. *Pathology & Genetics: Tumours of the Lung Pleura, Thymus and Heart.* Lyon: IARC Press; 2004. 128–36.
7. Meyerhoff RR, Yang CF, Speicher PJ, et al. Impact of mesothelioma histologic subtype on outcomes in the Surveillance, Epidemiology, and End Results database. *The Journal of surgical research.* 2015; 196:23–32. [PubMed: 25791825]
8. Herndon JE, Green MR, Chahinian AP, et al. Factors predictive of survival among 337 patients with mesothelioma treated between 1984 and 1994 by the Cancer and Leukemia Group B. *Chest.* 1998; 113:723–31. [PubMed: 9515850]
9. Pass HI, Giroux D, Kennedy C, et al. Supplementary prognostic variables for pleural mesothelioma: a report from the IASLC staging committee. *Journal of thoracic oncology : official publication of the International Association for the Study of Lung Cancer.* 2014; 9:856–64.

10. Kawashima A, Libshitz HI. Malignant pleural mesothelioma: CT manifestations in 50 cases. *AJR American journal of roentgenology*. 1990; 155:965–9. [PubMed: 2120965]
11. Gerbaudo VH, Katz SI, Nowak AK, et al. Multimodality Imaging Review of Malignant Pleural Mesothelioma Diagnosis and Staging. *PET clinics*. 2011; 6:275–97. [PubMed: 27156724]
12. Tyszko SM, Marano GD, Tallaksen RJ, et al. Best cases from the AFIP: Malignant mesothelioma. *Radiographics : a review publication of the Radiological Society of North America, Inc*. 2007; 27:259–64.
13. Alexander E, Clark RA, Colley DP, et al. CT of malignant pleural mesothelioma. *AJR American journal of roentgenology*. 1981; 137:287–91. [PubMed: 6789635]
14. Senyigit A, Bayram H, Babayigit C, et al. Malignant pleural mesothelioma caused by environmental exposure to asbestos in the Southeast of Turkey: CT findings in 117 patients. *Respiration; international review of thoracic diseases*. 2000; 67:615–22. [PubMed: 11124643]
15. Seely JM, Nguyen ET, Churg AM, et al. Malignant pleural mesothelioma: computed tomography and correlation with histology. *European journal of radiology*. 2009; 70:485–91. [PubMed: 18359180]
16. Dickens R, Ismail A, Martins R, et al. Mesothelioma: Can histological subtypes be differentiated on computer tomography? Scientific Poster Presentation at European Society of Thoracic Imaging. 2015
17. Husain AN, Colby T, Ordonez N, et al. Guidelines for pathologic diagnosis of malignant mesothelioma: 2012 update of the consensus statement from the International Mesothelioma Interest Group. *Archives of pathology & laboratory medicine*. 2013; 137:647–67. [PubMed: 22929121]
18. Bueno R, Reblando J, Glickman J, et al. Pleural biopsy: a reliable method for determining the diagnosis but not subtype in mesothelioma. *The Annals of thoracic surgery*. 2004; 78:1774–6. [PubMed: 15511473]
19. Kao SC, Yan TD, Lee K, et al. Accuracy of diagnostic biopsy for the histological subtype of malignant pleural mesothelioma. *Journal of thoracic oncology : official publication of the International Association for the Study of Lung Cancer*. 2011; 6:602–5.
20. Rusch VW, Gill R, Mitchell A, et al. A Multicenter Study of Volumetric Computed Tomography for Staging Malignant Pleural Mesothelioma. *The Annals of thoracic surgery*. 2016; 102:1059–66. [PubMed: 27596916]
21. Gill RR, Naidich DP, Mitchell A, et al. North American Multicenter Volumetric CT Study for Clinical Staging of Malignant Pleural Mesothelioma: Feasibility and Logistics of Setting Up a Quantitative Imaging Study. *Journal of thoracic oncology : official publication of the International Association for the Study of Lung Cancer*. 2016; 11:1335–44.
22. Kadota K, Kachala SS, Nitadori J, et al. High SUVmax on FDG-PET indicates pleomorphic subtype in epithelioid malignant pleural mesothelioma: supportive evidence to reclassify pleomorphic as nonepithelioid histology. *Journal of thoracic oncology : official publication of the International Association for the Study of Lung Cancer*. 2012; 7:1192–7.



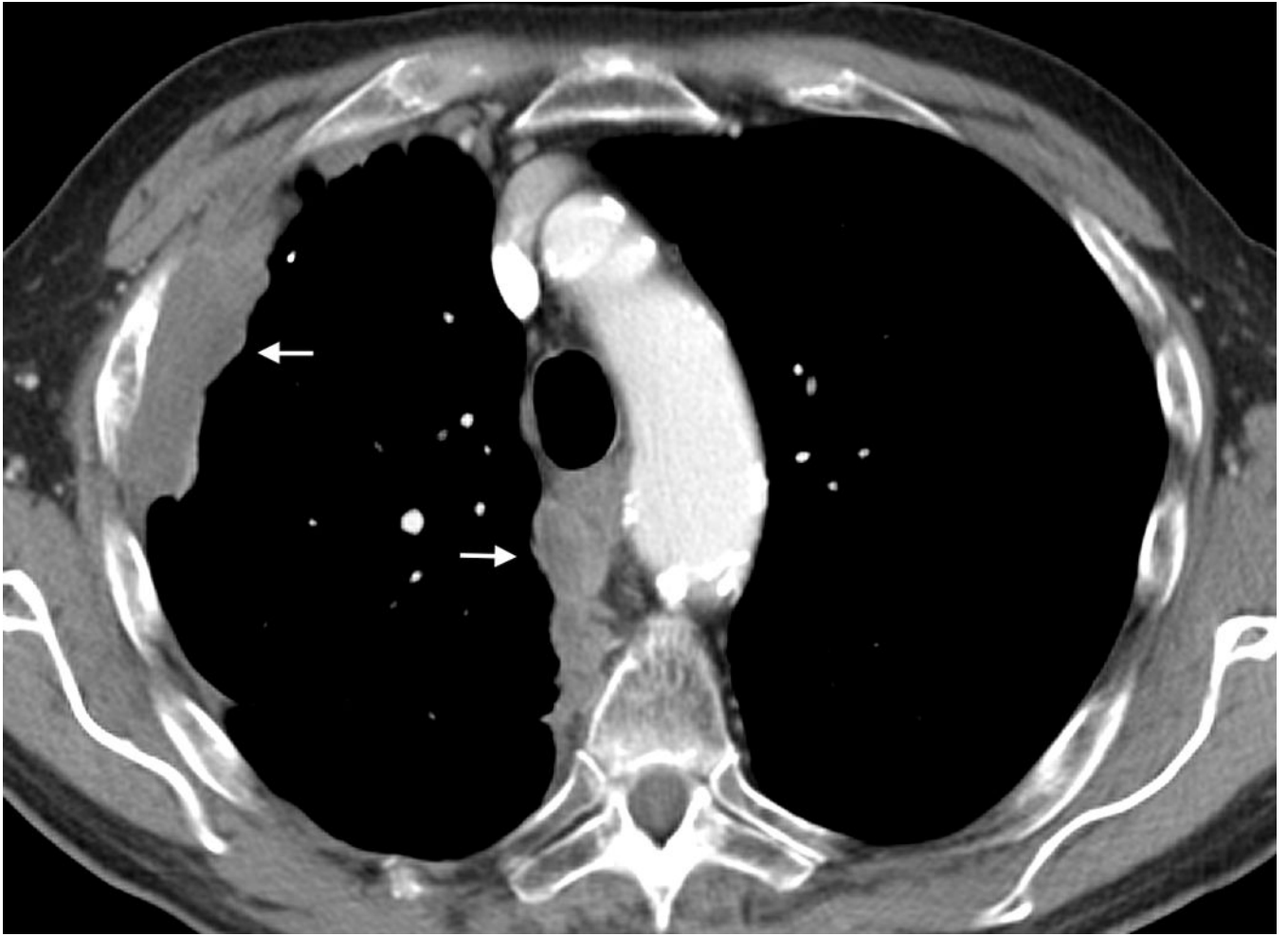
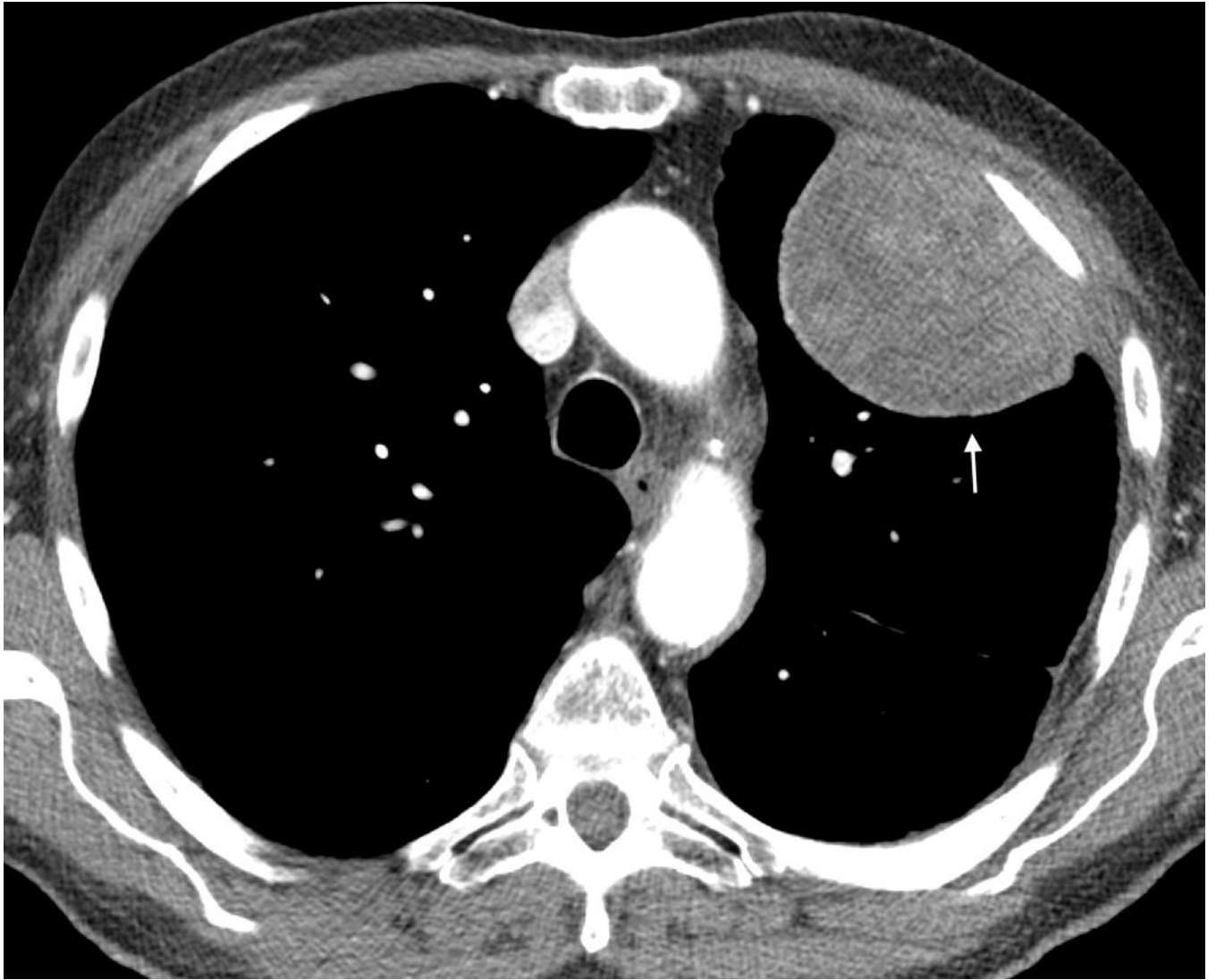


Figure 1.

A- Axial CT image of a 63 year old female with epithelioid mesothelioma demonstrating continuous pleural thickening (arrows), including the mediastinal pleura, and volume loss of the left hemithorax. B- Axial CT image of an 85-year-old male with biphasic mesothelioma demonstrating discontinuous pleural thickening (arrows), including involvement of the mediastinal pleura.



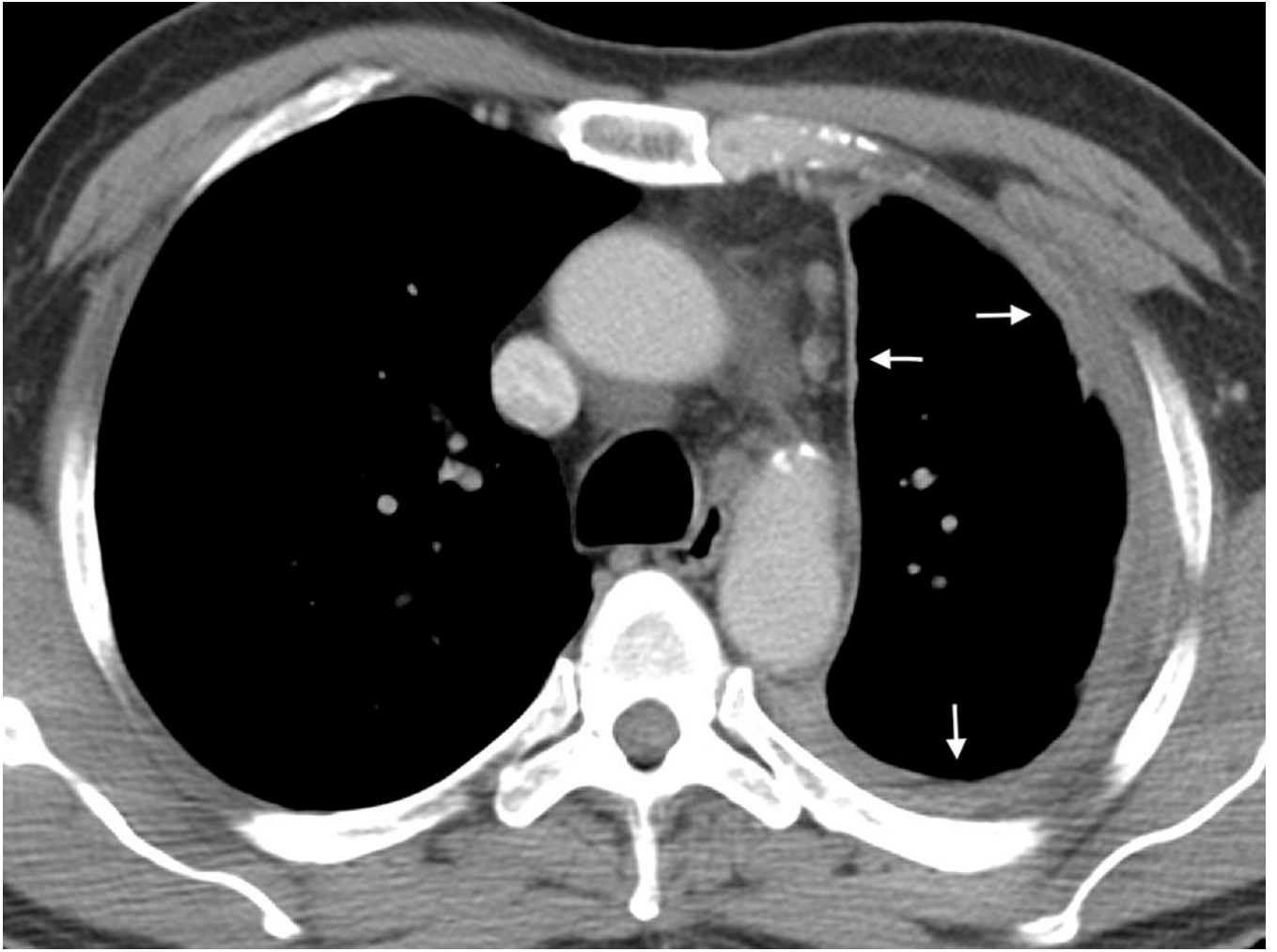


Figure 2.
A- Axial CT image of an 81 year old male with epithelioid mesothelioma demonstrating lobulated pleural thickening (arrow). B- Axial CT image of a 65 year old male with sarcomatoid mesothelioma demonstrating smooth pleural thickening (arrows).

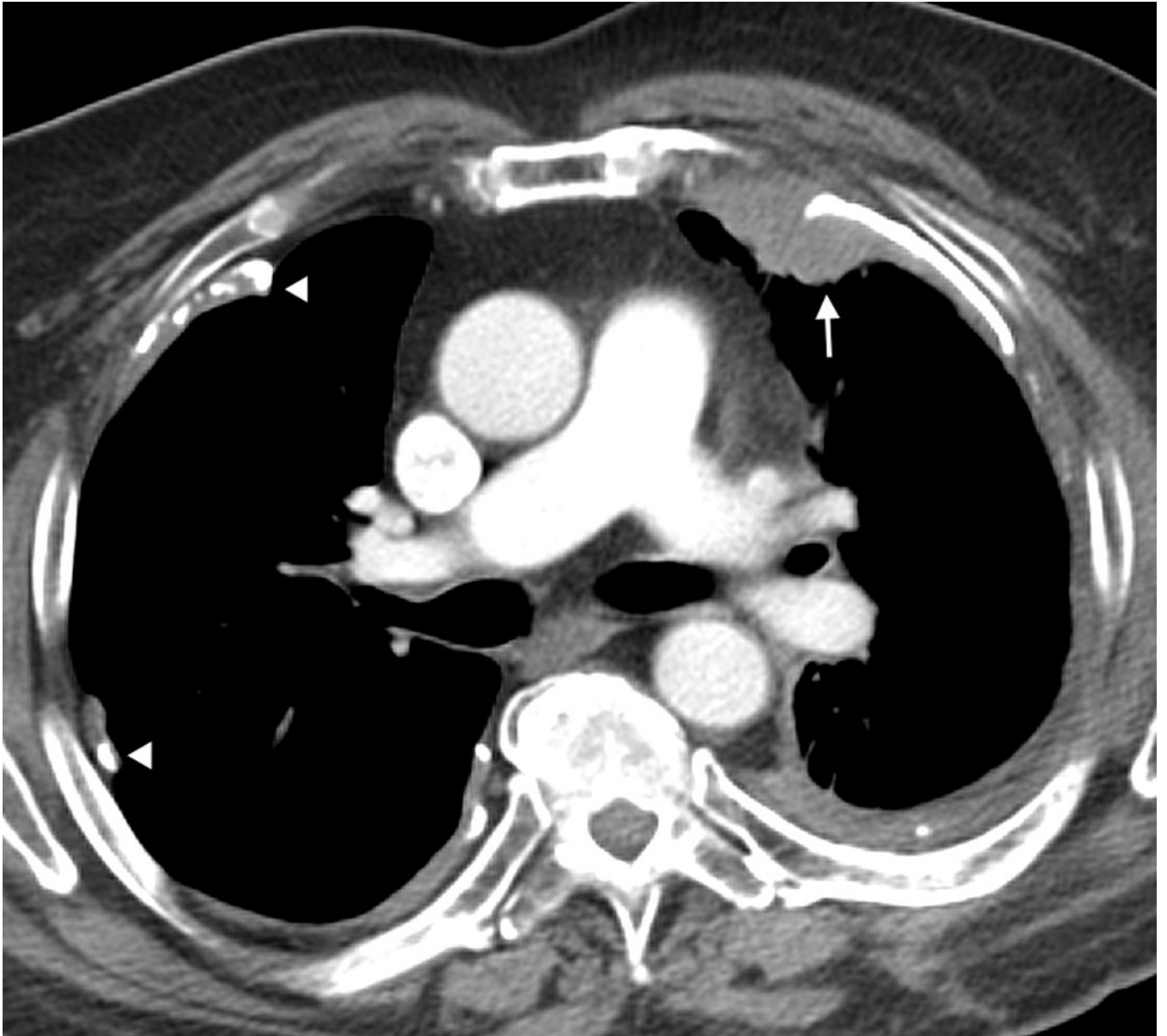


Figure 3. Axial CT image of a 73 year old male with epithelioid mesothelioma demonstrating calcified pleural plaques (arrow heads) and lobular pleural thickening (arrow).

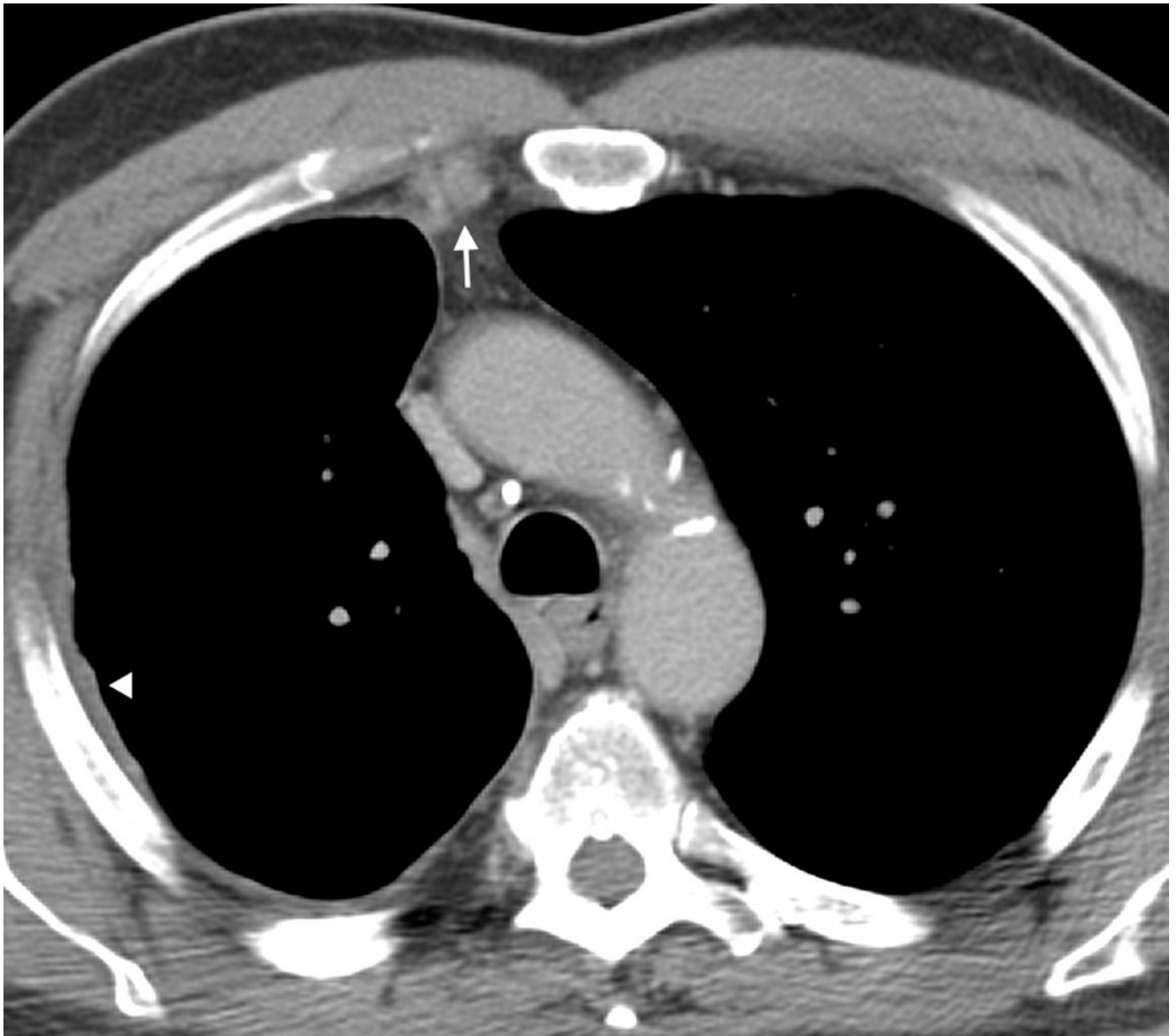


Figure 4. Axial CT image of a 78 year old male with epithelioid mesothelioma demonstrating enlarged internal mammary lymph nodes (arrow). Also noted is mild smooth pleural thickening (arrow heads).

Table 1
 Characterization of Pleural Thickening on CT – Comparing Epithelioid, Sarcomatoid, and Biphasic Subtypes

	Biphasic (N=17)	Epithelioid (N=97)	Sarcomatoid (N=11)	P-value	
Clinical Stage	1	1 (5.9%)	10 (10.3%)	2 (18.2%)	X
	2	5 (2.9%)	23 (23.7%)	4 (24.5%)	
	3	10 (58.8%)	48 (49.5%)	4 (24.5%)	
	4	1 (5.9%)	16 (16.5%)	1 (9.1%)	
Primary Affected Side	Right	7 (41.2%)	54 (55.7%)	5 (45.5%)	0.462
	Left	10 (58.8%)	43 (44.3%)	6 (54.5%)	
Maximum Pleural Location	Upper Lung	4 (26.7%)	23 (25.3%)	4 (40%)	0.740
	Lower Lung	8 (53.3%)	40 (44%)	3 (30%)	
	Diaphragm	3 (20%)	28 (30.8%)	3 (30%)	
	Lateral	9 (56.2%)	36 (39.6%)	7 (63.6%)	
Location of Maximum Pleural Thickness in the Upper Lobe	Mediastinal	5 (31.2%)	38 (41.8%)	3 (27.3%)	0.565
	Paraspinal	2 (12.5%)	17 (18.7%)	1 (9.1%)	
	Lateral	9 (56.2%)	49 (50.5%)	4 (40%)	
Location of Maximum Pleural Thickness in the Lower Lobe	Mediastinal	6 (37.5%)	32 (33%)	4 (40%)	0.812
	Paraspinal	1 (6.2%)	16 (16.5%)	2 (20%)	
	Continuous	8 (47.1%)	36 (37.1%)	6 (54.5%)	
Degree of Pleural Thickening	Discontinuous	9 (52.9%)	61 (62.9%)	5 (45.5%)	0.447
	Lobulated	16 (94.1%)	82 (84.5%)	10 (90.9%)	
Margin	Smooth	1 (5.9%)	15 (15.5%)	1 (9.1%)	0.721
	Maximum Upper Lung Pleural Thickness (mm)	10 (0 – 29)	9 (0 – 91)	11 (8 – 64)	
Maximum Lower Lung Pleural Thickness (mm)	11 (0 – 36)	14 (3 – 94)	16 (0 – 33)	0.763	
Maximum Diaphragmatic Pleural Thickness (mm)	12 (1 – 63)	11 (1 – 74)	13 (0 – 31)	0.983	

Table 2

Ancillary Findings on CT – Comparing Epithelioid, Sarcomatoid, and Biphasic Subtypes

	Biphasic (N=17)	Epithelioid (N=97)	Sarcomatoid (N=11)	P-value
Volume Loss	10 (58.8%)	44 (45.4%)	7 (63.6%)	0.393
Calcified Pleural Plaques	7 (41.2%)	24 (24.7%)	6 (54.5%)	0.075
Local Invasion (Any Location)	12 (70.6%)	50 (51.5%)	8 (72.7%)	0.216
Chest Wall Invasion	5 (29.4%)	18 (18.6%)	4 (36.4%)	0.267
Diaphragm Invasion	6 (35.3%)	31 (32%)	4 (36.4%)	0.841
Mediastinal Invasion	5 (29.4%)	37 (38.1%)	5 (45.5%)	0.683
Vascular Invasion	1 (5.9%)	9 (9.3%)	2 (18.2%)	0.552
Pleural Effusion	None	19 (19.6%)	4 (36.4%)	0.680
	Bilateral	0 (0%)	0 (0%)	
	Ipsilateral	14 (82.4%)	7 (63.6%)	
Pericardial Effusion	0 (0%)	9 (9.3%)	0 (0%)	0.367
Pulmonary Nodules	3 (17.6%)	12 (12.4%)	1 (9.1%)	0.888
Lymphadenopathy (Any Location) ^a	6 (35.3%)	29 (29.9%)	2 (18.2%)	0.651
Mediastinal Adenopathy ^a	6 (35.3%)	23 (23.7%)	1 (9.1%)	0.291
Ipsilateral Hilar Adenopathy ^a	2 (11.8%)	9 (9.3%)	1 (9.1%)	0.866
Contralateral Hilar Adenopathy ^a	0 (0%)	3 (3.1%)	0 (0%)	0.999
Axillary Adenopathy ^a	0 (0%)	2 (2.1%)	0 (0%)	0.999
Max Short Axis Diameter of Adenopathy	10 to 15 mm	5 (83.3%)	23 (79.3%)	0.999
	16 to 30 mm	1 (16.7%)	5 (17.2%)	
	> 30 mm	0 (0%)	1 (3.4%)	
Presence of Internal Mammary Nodes ^b	4 (23.5%)	21 (21.6%)	6 (54.5%)	0.071
Presence of Supra-diaphragmatic Nodes ^b	3 (17.6%)	23 (23.7%)	0 (0%)	0.174
Distant Metastases	0 (0%)	1 (1.1%)	0 (0%)	0.999

^a Adenopathy is defined as greater than 10 mm short axis.

^b Presence of any node regardless of size, including nodes less than 10 mm in short axis.